Original Article

Synergistic action of gemcitabine and celecoxib in promoting the antitumor efficacy of anti-programmed death-1 monoclonal antibody by triggering immunogenic cell death

Xiongjie Zhu[1#], Wenkai Zhang[1#], Zhongjian Yu[1], Xia Yang[1], Laiqing Li[2], Cuicui Chen[2], Temirbek Djumanazarov[3], David Piquemal[4], Abrorjon A. Yusupbekov[3], Yanfang Zheng[1^]

[1]Department of Medical Oncology, Affiliated Cancer Hospital and Institute of Guangzhou Medical University, Guangzhou, China; [2]Guangzhou Youdi Bio-Technology Co., Ltd., Guangzhou, China; [3]Republican Specialized Scientific and Practical Medical Center of Oncology and Radiology (National Cancer Center of Uzbekistan), Tashkent, Uzbekistan; [4]Acobiom, Montpellier, France

Contributions: (I) Conception and design: X Zhu, W Zhang; (II) Administrative support: AA Yusupbekov, Y Zheng; (III) Provision of study materials or patients: Z Yu, X Yang; (IV) Collection and assembly of data: L Li, C Chen, T Djumanazarov; (V) Data analysis and interpretation: X Zhu, W Zhang; (VI) Manuscript writing: All authors; (VII) Final approval of manuscript: All authors.

[#]These authors contributed equally to this work.

Correspondence to: Yanfang Zheng, MD. Department of Medical Oncology, Affiliated Cancer Hospital and Institute of Guangzhou Medical University, 78 Hengzhigang Road, Guangzhou 510095, China. Email: zheng2020@gzhmu.edu.cn; Abrorjon A. Yusupbekov, MD. Republican Specialized Scientific and Practical Medical Center of Oncology and Radiology (National Cancer Center of Uzbekistan), 383 Farobi Street, Tashkent 100052, Uzbekistan. Email: dr.abr_info@mail.ru.

Background: Emerging evidence suggests that immunogenic chemotherapy not only kills tumor cells but also improves the immune-suppressive tumor microenvironment by inducing immunogenic cell death (ICD), leading to sustained anti-tumor effects. The lack of ICD inducers explored in lung cancer necessitates investigation into new inducers for this context, therefore, this study aims to explore whether the gemcitabine (GEM) and celecoxib can activate the immunogenic chemotherapy progress in lung cancer tissue.

Methods: We assessed five chemotherapeutic agents for their ability to trigger ICD using *ex vivo* and *in vivo* experiments, including western blotting (WB), flow cytometry, and tumor preventive vaccine assays. Additionally, we evaluated the synergistic effects of GEM, celecoxib, and anti-programmed death 1 monoclonal antibody (aPD-1) in tumor-bearing mice to understand how GEM activates antitumor immunity and enhances immunochemotherapy.

Results: GEM was identified as an effective ICD inducer, showing high expression of calreticulin (CRT) and heat shock protein 90 (HSP90). Co-culture with GEM-treated cells [Lewis lung carcinoma (LLC) and CMT-64] enhanced dendritic cell (DC) activity, evidenced by maturation markers and increased phagocytic capacity. Moreover, celecoxib was found to enhance ICD by reducing indoleamine 2,3-dioxygenase 1 (IDO1) expression and increasing reactive oxygen species (ROS)-based endoplasmic reticulum (ER) stress. The combination therapy [GEM, celecoxib, and aPD-1 (GCP)] exhibited potent and sustained antitumor activity in immunocompetent mice, with enhanced recruitment of tumor-infiltrating lymphocytes.

Conclusions: These findings support the potential use of GCP therapy as a treatment option for lung cancer patients.

Keywords: Immunochemotherapy; tumor microenvironment; immunogenic cell death (ICD); lung cancer

Submitted Apr 27, 2024. Accepted for publication Jun 24, 2024. Published online Jun 27, 2024.
doi: 10.21037/tcr-24-698
View this article at: https://dx.doi.org/10.21037/tcr-24-698

^ ORCID: 0000-0002-5591-6425.

Introduction

Immunogenic cell death (ICD) is a particular form of cell death that is triggered by certain chemotherapeutic agents, radiotherapy, or photodynamic therapy (1). A feature of ICD is the presence of damage-associated molecular patterns (DAMPs), including calreticulin (CRT), high mobility group box-1 (HMGB1), adenosine triphosphate (ATP), heat shock protein 70 (HSP70), heat shock protein 90 (HSP90), and type 1 interferons (IFNs). Translocation of CRT to the cell surface acts as an effective "eat me" signal, interacting with CD91 receptors on phagocytes in the immunogenic tumor medium to efficiently activate the phagocytosis of the dying cells (2). HMGB1 is a powerful cytokine that can attract various immune cells and induce maturation of dendritic cells (DCs) (3). ATP, an effective "find me" signal that can also function as an adjuvant of the antitumor immune response, is detected by purinergic receptors (P2RX7) on DCs (2). Recently, Legrand and colleagues proposed that ICD should be defined as a type of regulated cell death that results from successful dialog between the dying cells and an appropriately disposed immune system (4).

Immunogenetic chemotherapy (IC) is a special type of chemotherapy that use drugs that can induce ICD (5). One such drug is doxorubicin (DOX), which is a known inducer of ICD that enables transformation of immune "cold" tumors to "hot" tumors (6). In addition, some non-ICD inducers are able to induce ICD with the assistance of other agents. For example, the acknowledged non-ICD inducer cisplatin can induce ICD when coadministered with digoxin (7). Mechanistically, the tumor microenvironment, including that of lung and breast cancer, is characterized by high expression of cyclooxygenase-2 (COX-2) and its product, prostaglandin E2 (PGE2) (8,9). Furthermore, PGE2 can dampen the function of T cells and T helper (Th) lymphocytes by initiating the production of immunosuppressive cytokines and molecules such as indoleamine 2,3-dioxygenase 1 (IDO1) (10). The overexpression of IDO1 can contribute to this detrimental effect by metabolizing the essential amino acid tryptophan into tyrosine, which is an effective T-cell metabolic inhibitor that inhibits T-cell proliferation (11). One study demonstrated that the COX-2 inhibitor celecoxib could enhance the efficacy of a breast cancer vaccine (12). Recent findings have spurred us to investigate the treatment of lung cancer using a combination of gemcitabine (GEM) and celecoxib.

Currently, resistance to chemotherapy in patients with advanced lung cancer is still a huge problem for clinicians, and we aim to explore a therapeutic agent or regimen that can delay chemotherapy resistance and improve survival prognosis. we hypothesized that the combination of IC agents and anti-programmed death 1 monoclonal antibody (aPD-1) might achieve more efficacious antitumor immunotherapy. In this study, we first demonstrated that GEM is an inducer of ICD. We subsequently examined the synergistic antitumor efficacy of GEM-celecoxib combination therapy *in vitro* and *in vivo*. Furthermore, we tested the effects of this combination therapy on treatment with aPD-1. Our findings suggested a favorable antitumor effect of the combination of GEM, celecoxib, and aPD-1 (GCP). Mechanistically, we demonstrated that celecoxib inhibits IDO1 expression by suppressing the PI3K/AKT signaling pathway, thus enhancing the induction of ICD by GEM *in vitro*. Overall, our results should facilitate the development of IC strategies that may prove to be superior alternatives for cancer therapy. We present this article in accordance with the ARRIVE and MDAR reporting checklists (available at https://tcr.amegroups.com/article/view/10.21037/tcr-24-698/rc).

Highlight box

Key findings

- In the present study, we found that the combination therapy of gemcitabine (GEM), celecoxib, and anti-programmed death 1 monoclonal antibody (aPD-1) exhibited potent antitumor activity in immunocompetent mice via synergistic antitumor activity and recruitment of tumor-infiltrating lymphocytes.

What is known and what is new?

- GEM and celecoxib have been proven to exert antitumor effects.
- GEM can promote the infiltration of $CD8^+$ T cells in the tumor microenvironment by stimulating immunogenic cell death (ICD) in lung cancer cells while celecoxib can enhance the ICD effect of GEM by inhibiting the expression of indoleamine 2,3-dioxygenase 1. Ultimately, the combination of GEM and celecoxib can enhance the antitumor immune effect of aPD-1.

What is the implication, and what should change now?

- These results support a combination of GEM, celecoxib, and aPD-1 as a potential treatment regimen for patients with lung cancer. However, a large number of clinical studies are still needed to validate this approach before it can be applied in clinic.

Methods

Cell lines and cell culture

The murine lung cancer cell lines [Lewis lung carcinoma

(LLC) and CMT-64] derived from C57 BL/6J mice were purchased from Jennio Biotech Co., Ltd. (Guangzhou, China). LLC cells were cultured in Dulbecco's Modified Eagle Medium supplemented with 10% fetal bovine serum (FBS) and 1% penicillin-streptomycin (100 U/mL). CMT-64 cells were cultured in RPMI 1640 supplemented with 10% FBS and 1% penicillin-streptomycin (100 U/mL).

Western blotting (WB)

Pretreated CMT-64 and LLC cells were washed with phosphate-buffered saline (PBS) and lysed in radioimmunoprecipitation assay (RIPA) buffer containing 1% proteinase and phosphatase inhibitor. Total protein was extracted from the lysates and quantified using a bicinchoninic acid (BCA) kit (Beyotime, Shanghai, China). A 50-μg protein sample was used for the immunoblotting assay. After incubation with primary antibodies, including glyceraldehyde-3-phosphate dehydrogenase (GAPDH; 60004-1-Ig), HSP90 (60318-1-Ig; Proteintech, Rosemont, IL, USA), COX-2 (12282), IDO1, (86630), AKT (4685), phospho-AKT (P-AKT; 4060), PI3K (4257), phospho-PI3K (P-PI3K; 4228), Bip (3177), CHOP (2895), CRT (12238) [Cell Signaling Technology (CST), Danvers, MA, USA], and Bcl-2 (BS70205; Bioworld Technology, Bloomington, MN, USA), the immunoreaction was visualized using an enhanced chemiluminescence (ECL) kit. The above experimental method was repeated three times.

In vitro apoptosis assay

A total of 30×10^5 cells (LLC and CMT-64) were cultured in a six-well plate and treated with dimethyl sulfoxide (DMSO), GEM (2 μg/mL), and celecoxib (40 μM) for 24 h. Cells floating in the supernatants and cells on the culture plate were collected and then washed with PBS. The cells were incubated with the prepared working solution [annexin V-fluorescein isothiocyanate (FITC) and propidium iodide (PI)] in the dark for 15 min and then analyzed via flow cytometry.

Determination of reactive oxygen species (ROS)

The levels of ROS in cells were determined using a 2,7-dichloro-dihydro-fluorescein diacetate (DCFH-DA) probe (S0033M; Beyotime, Beijing, China). According to the manufacturer's instructions, treated-cells were collected and washed with culture medium. The cells were incubated with prepared working solution in the dark for 20–30 min and then analyzed via flow cytometry.

Extraction of mouse bone marrow-derived DCs

DCs were generated from female C57 BL/6J mice and cultured in RPMI 1640 supplemented with 10% FBS, 1% penicillin-streptomycin (100 U/mL), interleukin (IL)-4 (5 ng/mL), and granulocyte-macrophage colony-stimulating factor (GM-CSF; 10 ng/mL).

DC phagocytosis

Briefly, 5×10^5 mouse-derived lung cancer cells (LLC and CMT-64) were stained with a CytoTrace Red Fluorescent Probe (40717ES50; Yeasen Biotechnology, Shanghai, China), and 5×10^5 DCs were stained with CellTracker Green CMFDA (40721ES50; Yeasen Biotechnology). The pretreated cells [group: DMSO, docetaxel (DTX), DOX, pemetrexed (PEM), GEM, and navelbine (NVB)] were cocultured with DCs for 24 h to investigate phagocytosis during incubation. The collected cells were analyzed via flow cytometry. The above experimental method was repeated three times.

Transcriptome sequencing

A total of 5×10^5 LLC cells were pre-seeded in 6 cm dishes, and treat them with PBS and GEM for 24 h, respectively, after the cells were fully walled. Finally, extract RNA using Trizol and conduct quality evaluation. Subsequently, RNA reverse transcription, library establishment, and library sequencing were performed using Illumina bcl2fastq Conversion Software (v2.20.0.422) to convert the data format and Trimmomatic PE (v0.39) for quality control. The sequencing data were finally analyzed by Kyoto Encyclopedia of Genes and Genomes (KEGG).

Flow cytometry

Spleen cells were extracted from treated mice, and red blood cells were removed using an erythrocyte lysis buffer (Biosharp, Hefei, China). The spleen cells were then probed with the following primary antibodies: Pharmingen PE hamster anti-mouse CD11c (557401; BD Biosciences, Franklin Lakes, NJ, USA), CD86/B7-2 (GL-1) rat monoclonal antibody (FITC conjugate; 99879; CST), APC anti-mouse I-A/I-E (107613), Brilliant Violet 421 anti-

mouse/human CD11b (101235), PerCP/Cyanine5.5 anti-mouse Ly-6G/Ly-6C (Gr-1; 108427), Brilliant Violet 42 anti-mouse CD3ε (100341), PE anti-mouse CD8a (100707), PE/cyanine7 anti-mouse IFN-γ (505825), FITC anti-mouse CD4 (100405), Alexa Fluor 647 anti-mouse FOXP3 (126407), PE anti-mouse CD62L (104407), and PerCP/Cyanine5.5 anti-mouse/human CD44 (103031; BioLegend; San Diego, CA, USA). For staining of intracellular FOXP3 and IFN-γ, fixation buffer (420801) and intracellular staining permeabilization wash buffer (10×; 421002; BioLegend) were used. The specific experimental procedures were the same as those used in a previous study (12). Data were acquired on a flow cytometer (CytoFLEX, Beckman Coulter, Brea, CA, USA) and analyzed using the FlowJo software (BD Biosciences). The above experimental method was repeated three times.

Immunohistochemistry (IHC)

Tissue specimens were collected and fixed with 10% formalin solution. The specimens were processed using an automatic tissue dehydrator and embedded in paraffin using an embedding machine (Tissue-Tek, Sakura Finetek, Torrance, CA, USA). The tissue sections (4 μm) were stained with hematoxylin and eosin (HE) to further analyze proteins of interest. The specific procedures were as follows: after dewaxing in xylene and hydration with an alcohol gradient (100% for 5 min, 95% for 5 min, 85% for 5 min, and 75% for 5 min), endogenous peroxidase activity was blocked via incubation with 2% H_2O_2, and then antigen retrieval was conducted by microwaving in 10 mM of citrate buffer for 15 min at 95 ℃. Sections were then incubated with primary antibodies, including COX-2 (1:500; 12282; CST), PD-1 (1:200; 84651; CST), IDO1 (1:200; 13268-1-AP; Proteintech), and CD8 (1:100; AF5126; Affinity, Eden Prairie, MN, USA), overnight at 4 °C. Streptavidin-linked secondary antibody (LSAB+ kit, Dako, Agilent Technologies, Santa Clara, CA, USA) was applied for 30 min, which was followed by application streptavidin peroxidase for 15 min. After incubation for 5 min in the substrate developer, counterstaining with hematoxylin was conducted for 3 min.

Mouse cytokine enzyme-linked immunosorbent assay (ELISA)

Mouse cytokine (IL-1β, IFN-γ, and HMGB1) ELISA kits were used to estimate levels of these cytokines in supernatants of samples from *in vivo* or *in vitro* experiments. Initially, the collected supernatants were centrifuged to remove impurities and incubated on the enzyme plate for 90 min. The plate was washed with buffer (5×) and incubated with biotin-labeled antibodies at 37 ℃ for 60 min. Subsequently, horseradish peroxidase enzyme conjugates were added and incubated in the dark for 30 min after washing. Finally, the reaction was terminated, and the absorbance at 450 nm was recorded on a microplate reader.

Tumor-prevention vaccine experiment

This study was performed at Zhujiang Hospital of Southern Medical University. All animal experiments were approved by the Animal Care and Use Committee of Southern Medical University (No. LAEC-2020-049). The welfare of live experimental animals was maintained in strict accordance with the Ministry of Science and Technology (2006) No. 398 Guidelines for the Treatment of Experimental Animals for the care and use of animals. A protocol was prepared before the study without registration. 18 C57 BL/6J female mice weighing 20 g (purchased from Guangdong Provincial Laboratory Animal Center and Southern Medical University Laboratory Animal Center) aged 6–7 weeks were bred in a specific pathogen-free (SPF) animal experiment center (two C57 BL/6J mice were excluded by accidental death). LLC cells were treated with PBS, GEM, or DOX, and then the flanks of C57 BL/6J mice were inoculated subcutaneously with 1×10^6 dying cells. The PBS-treated cells were frozen and thawed as the control group and DOX-treated cells acted as the positive group. After 7 days, 5×10^5 LLC cells were injected into the contralateral armpit, which was monitored every 3 days. Prevention was considered to have failed if a palpable subcutaneous tumor could be detected.

Mouse ectopic model of lung cancer

To investigate the inhibitory efficacy of a GCP in mice bearing a lung cancer xenograft and to further evaluate whether there was any long-lasting antitumor immunity, 35 C57 BL/6J mice (6–7 weeks old) were divided into five groups [PBS, GEM, aPD-1, GEM + celecoxib (GC), and GCP]. LLC cells (5×10^5) were subcutaneously inoculated into the armpit or the leg. Therapeutic drugs (GEM: 25 mg/kg; aPD-1: 100 μg/mouse) as described above were injected via the tail vein when the tumor volume reached approximately 100–150 mm^3. Celecoxib (50 mg/kg) was administered by gavage. Tumor volumes were monitored using an electronic vernier caliper every 2 days. Tumor volume was calculated as

follows: volume (mm^3) = length × width × width/2.

Cell depletion assay

Cell depletion was conducted to investigate the specific cell type involved in antitumor immunity. For removal of $CD4^+$ and $CD8^+$ T cells, anti-CD4 (100 μg/mouse; BE0003) and anti-CD8 (100 μg/mouse; BE0061) were injected via the tail vein 1 day before commencement of chemotherapy and then every 2 days thereafter. The DMSO group was used as a control group, and tumor growth was monitored every 2 days. Depletion of $CD4^+$ and $CD8^+$ T cells was determined via flow cytometry.

Lung metastasis model of lung cancer

Subcutaneous tumors were induced in 6- to 8-week-old C57 BL/6J mice and treated three times with GCP. Frozen and thawed LLC cells were injected subcutaneously into the armpit as the control (PBS) group. Next, parental LLC cells (2×10^5) were injected via the tail vein. The mice were anesthetized and euthanized 30 days postinjection. Subsequently, the lungs were obtained and stained with HE. Representative results were photographed and recorded using an optical microscope.

Statistical analysis

Data analyses were performed using SPSS 22.0 (IBM Corp., Armonk, NY, USA), and data are expressed as the mean ± standard error of the mean (SEM). Statistical significance was assessed with the two-tailed unpaired Student *t*-test. P values <0.05 were considered to be statistically significant.

Results

GEM as an inducer of ICD

To determine whether a chemotherapy drug could induce ICD, WB, ELISA, DC phagocytosis, and activation assays were performed. As indicated from the WB results (*Figure 1A*), GEM and DOX (positive control) enhanced expression of CRT and HSP90. According to the ELISA data, although the levels of HMGB1 increased from the DMSO, DOX, to the GEM groups, respectively (*Figure 1B*), this difference was not significant. Because activation of DCs is a feature of ICD, we tested the DC activation and rates of phagocytosis after treatment with chemotherapeutic drugs. Almost all groups exhibited enhanced phagocytosis and a greater activation of DCs [$CD11c^+$major histocompatibility complex (MHC)-II^+] with the exception of the DTX group (*Figure 1C,1D* and Figure S1A,S1B). The effects of DTX (negative control), DOX (positive control), and GEM (our ICD inducer) on the expression of CRT and HSP90 were also examined. Impressively, GEM enhanced the expression of CRT and HSP90 in a time- and concentration-dependent manner within a certain concentration and time range (*Figure 1E,1F* and Figure S1C-S1F). Interestingly, in the LLC and CMT-64 cells pretreated with GEM, we found the high expression of CRT, ATP, and some chemokines (CCL5, CXCL3, and CXCL10) (Figure S1G,S1H), which are known to have important roles in the recruitment of infiltrating T lymphocytes (TILs).

Consequently, we found that three mice in the PBS group developed palpable subcutaneous tumors by day 4, and all eight mice had obvious tumors on day 7 as confirmed by the *in vivo* prophylactic vaccine experiments (*Figure 1G*). In comparison, GEM protected most of the mice (6/8) from reinvasion of tumor cells (*Figure 1H*) over 28 days. In addition, analysis of the immune cells in the spleen revealed no significant differences in the numbers of $CD3^+CD4^+$ or $CD3^+CD8^+$ T cells among the groups (*Figure 1I,1J*), but there were more $CD3^+IFN\text{-}\gamma^+$ T cells in the GEM and DOX groups (*Figure 1K*). Consistent with our *in vitro* data, GEM and DOX were found to activate DCs (*Figure 1L*). Moreover, we found that the proportion of memory T cells ($CD3^+CD4^+CD62L^-$) in the GEM and DOX groups was significantly increased compared with that in the PBS group (*Figure 1M*). These results suggest that GEM acted as an inducer of ICD via stimulation of DAMPs and release of chemokines, leading to the attraction and activation of immune cells against tumors.

Celecoxib enhanced the cellular immunogenicity induced by GEM

Although GEM can promote the expression of DAMPs in dying cells, it also increases the expression of PGE2, which is an inhibitory DAMP that can suppress the ICD effect induced by GEM. As shown in *Figure 2A*, although there was no significant difference between the celecoxib and DMSO groups, there was a slight decrease in the levels of PGE2 in the celecoxib group. Meanwhile, a ROS probe (DCFH-DA) was used to track the levels of ROS induced by GEM or celecoxib. Unexpectedly, celecoxib enhanced the ROS production stimulated by GEM (*Figure 2B,2C* and Figure S2A,S2B). Additionally, analysis of the apoptosis state via flow cytometry

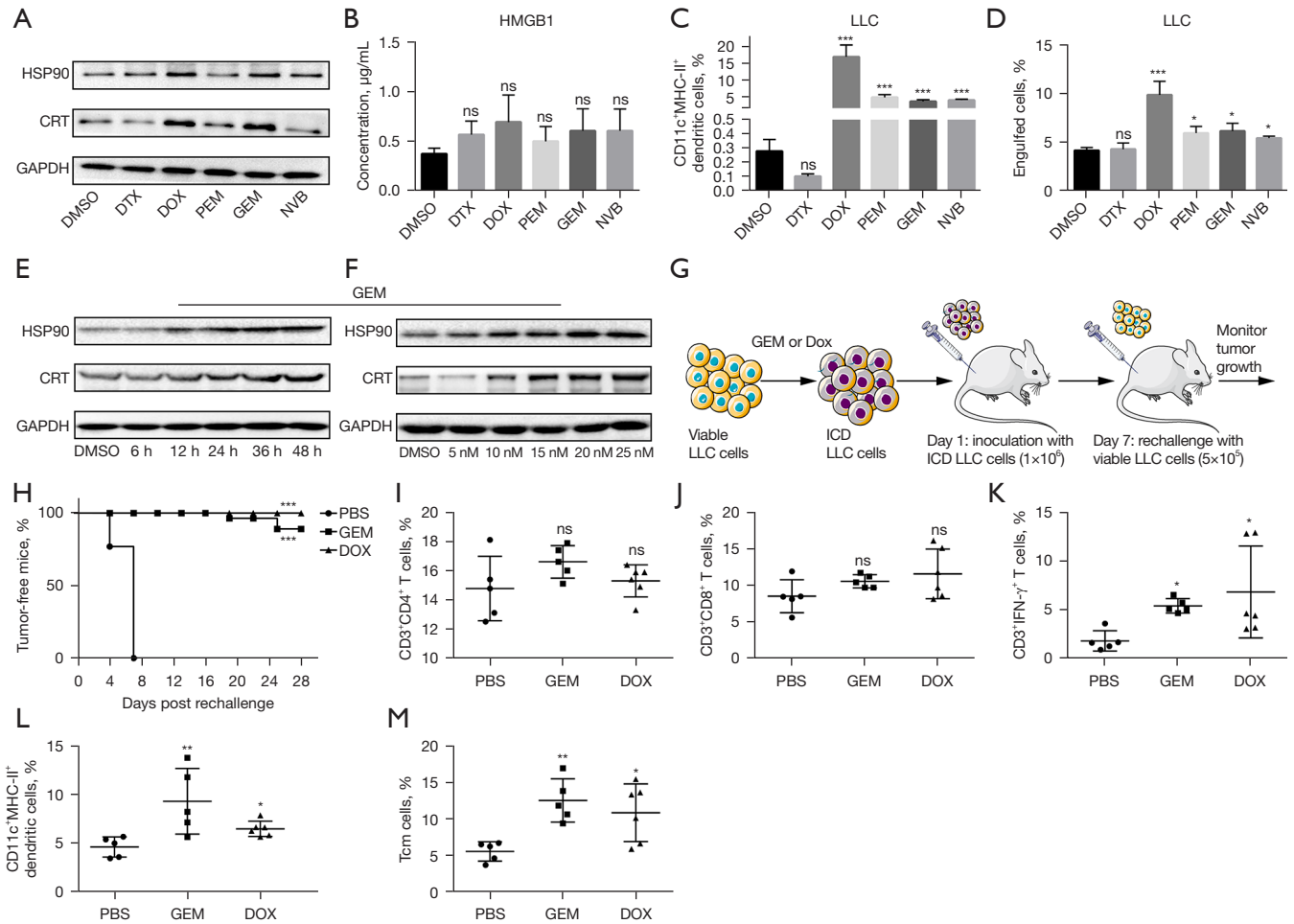

Figure 1 GEM induced lung cancer cell immunogenicity. (A) LLC cells were treated with various chemotherapeutic agents (DTX, DOX, PEM, GEM, and NVB) for 24 h, and WB was used to measure levels of DAMPs (CRT and HSP90). (B) Analysis of HMGB1 was performed via ELISA. (C,D) The activation of DCs was determined by measuring the percentage of mature DCs and phagocytosis using flow cytometry after coculture of treated cancer cells with DCs. (E,F) Time- and concentration-dependent production of DAMPs were evaluated via WB. (G) The specific procedure for the prophylactic tumor vaccine. (H) The percentage of tumor-free mice was monitored. (I-M) The levels of $CD4^+$ ($CD3^+CD4^+$), $CD8^+$ ($CD3^+CD8^+$) T cells, $CD3^+IFN\text{-}\gamma^+$ T cells, mature DCs ($CD11c^+MHC\text{-}II^+$), and Tcm cells ($CD3^+CD4^+CD62L^-$) were analyzed via flow cytometry. *, P<0.05, ***, P<0.001, compared with the DMSO group; **, P<0.01, compared with PBS group; ns, P>0.05. HSP90, heat shock protein 90; CRT, calreticulin; GAPDH, glyceraldehyde-3-phosphate dehydrogenase; DMSO, dimethyl sulfoxide; DTX, docetaxel; DOX, doxorubicin; PEM, pemetrexed; GEM, gemcitabine; NVB, navelbine; HMGB1, high mobility group box-1; LLC, Lewis lung carcinoma; ICD, immunogenic cell death; IFN, interferon; MHC, major histocompatibility complex; Tcm, central memory T; WB, western blotting; DAMPs, damage associated molecular patterns; ELISA, enzyme-linked immunosorbent assay; DCs, dendritic cells.

was consistent with the assumption that celecoxib could increase the antitumor effect of chemotherapeutic agents (*Figure 2D,2E* and Figure S2C,S2D) (13). Both GEM and celecoxib accelerated the apoptosis of cancer cells, and addition of celecoxib to the GEM group increased tumor-suppression efficiency.

Next, KEGG pathway analysis was conducted and revealed that the major pathways of GEM-treated cells included cell growth and death, signal transduction, folding, sorting and degradation, and the immune system (*Figure 2F*). Subsequently, we used WB to examine the expression of endoplasmic reticulum (ER) stress-related

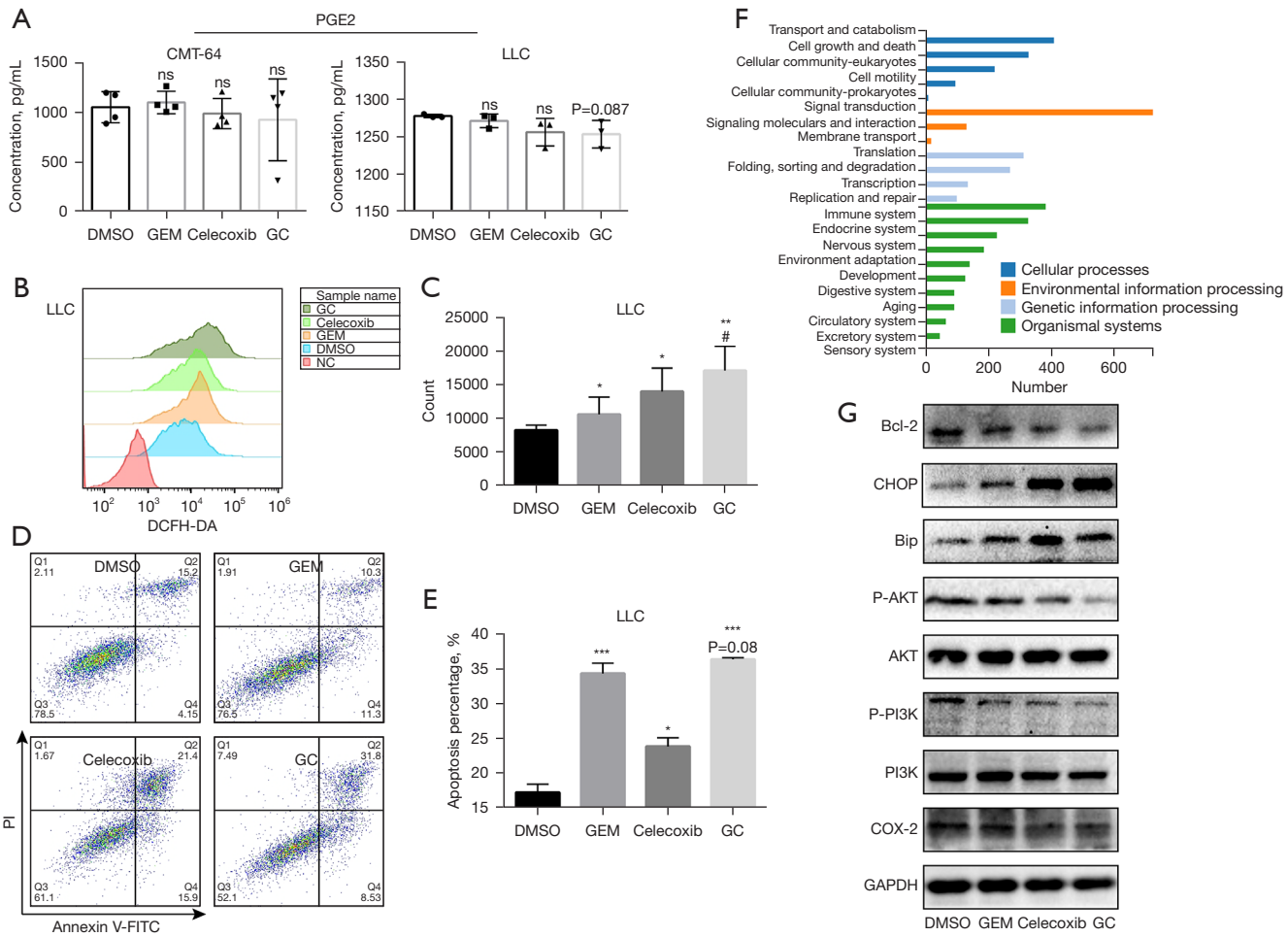

Figure 2 Combination therapy with GEM and celecoxib influenced biological function *in vitro*. (A) The effect of GEM and celecoxib on production of PGE2. (B,C) ROS levels and (D,E) apoptosis were determined via flow cytometry. (F) Lung cancer cells (LLC and CMT-64) were treated with DMSO and GEM for 24 h, which was followed by KEGG pathway analysis of GEM-treated cells conducted via transcriptome sequencing. (G) Expression of PI3K/AKT pathway, ER stress-related proteins (CHOP and Bip), and Bcl-2. *, P<0.05, **, P<0.01, ***, P<0.001, compared with the DMSO group; #, P<0.05, GC group compared with the GEM group; ns, P>0.05. PGE2, prostaglandin E2; LLC, Lewis lung carcinoma; DMSO, dimethyl sulfoxide; GEM, gemcitabine; GC, GEM + celecoxib; DCFH-DA, 2,7-dichloro-dihydro-fluorescein diacetate; NC, normal control; FITC, fluorescein isothiocyanate; PI, propidium iodide; P-, phospho-; COX-2, cyclooxygenase-2; GAPDH, glyceraldehyde-3-phosphate dehydrogenase; ROS, reactive oxygen species; KEGG, Kyoto Encyclopedia of Genes and Genomes; ER, endoplasmic reticulum.

proteins (Bip and CHOP), antiapoptotic protein (Bcl-2), and other proteins (COX-2 and PI3K/AKT signaling pathway) (*Figure 2G* and Figure S2E). Treatment of cells (CMT-64 and LLC) with GEM and celecoxib promoted the production of Bip and CHOP. In addition, COX-2 was inhibited by the addition of celecoxib. Decreased levels of P-PI3K and P-AKT indicated that the PI3K/AKT signaling pathway was inactivated by GEM and celecoxib. Moreover, Bcl-2 expression was downregulated after treatment with GEM, celecoxib alone, or their combination. Altogether, the results suggested that GEM- or celecoxib-treated cells may be subject to apoptosis and ER stress-mediated by the PI3K/AKT signaling pathway.

Combination therapy with GEM and celecoxib enhanced the activation of DCs

As the combination of GEM and celecoxib is a powerful

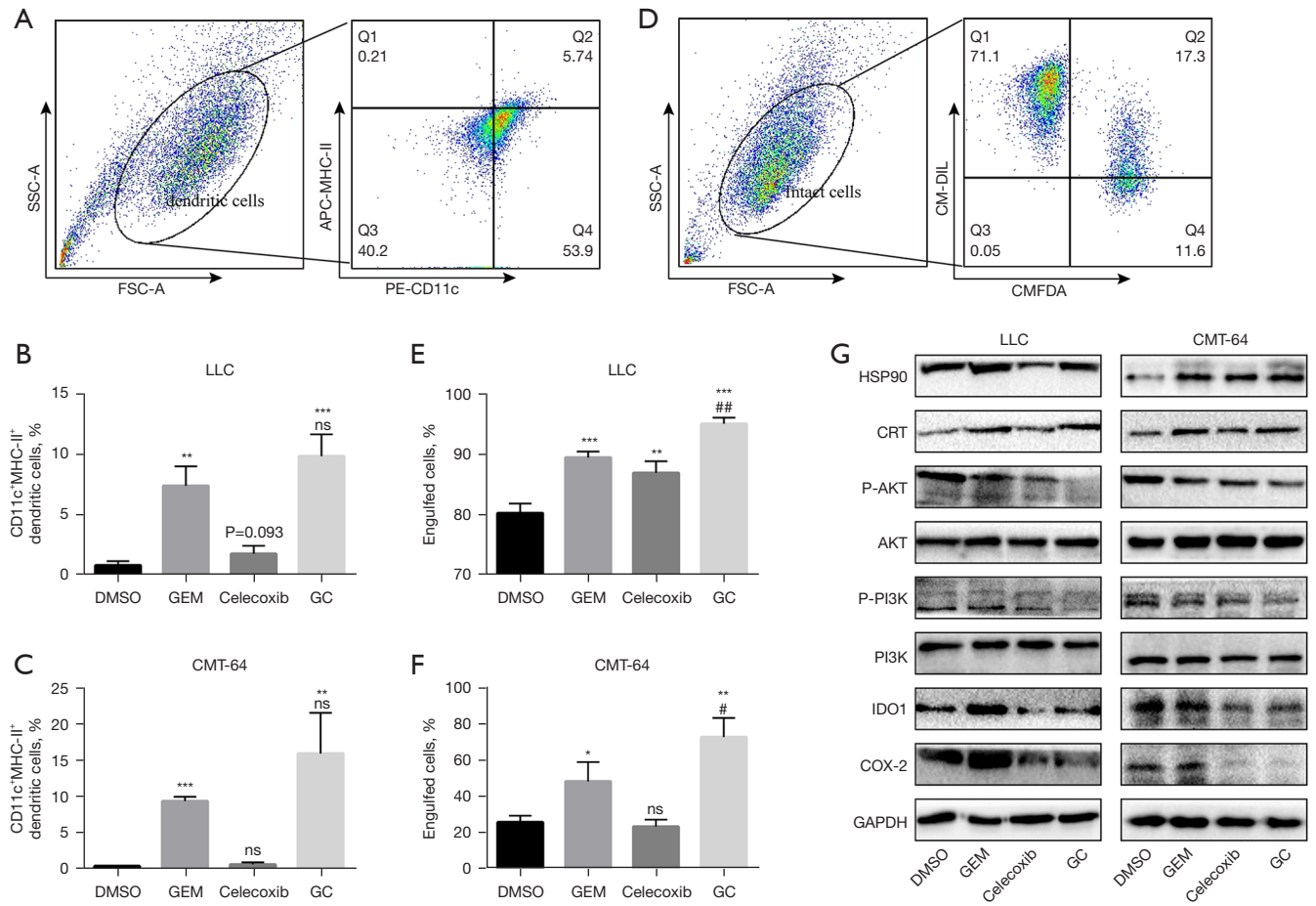

Figure 3 Celecoxib promoted the processing of cells treated with GEM. Flow cytometry analysis of (A) mature and (D) phagocytic DCs. (B,C) Changes in activation state of DCs after cocultured with pretreated cells for 24 h. (E,F) Pretreated cells stained with CytoTrace Red Fluorescent Probe cocultured with CellTracker Green CMFDA in the dark for 24 h, which was followed by flow cytometry analysis of double-labeled cells. (G) PI3K/AKT pathway (PI3K, P-PI3K, AKT, and P-AKT) protein, DAMP (CRT and HSP90), COX-2, and IDO1 expression (G). *, P<0.05, **, P<0.01, ***, P<0.001, compared with the DMSO group; #, P<0.05, ##, P<0.01, GC group compared with the GEM group; ns, P>0.05. SSC, side scatter; FSC, forward scatter; APC, allophycocyanin; MHC, major histocompatibility complex; PE, polyethylene dye; LLC, Lewis lung carcinoma; DMSO, dimethyl sulfoxide; GEM, gemcitabine; GC, GEM + celecoxib; CM-DIL, cell membrane staining reagent; CMFDA, 5-chloromethylfluorescein diacetate; HSP90, heat shock protein 90; CRT, calreticulin; P-, phospho-; IDO1, indoleamine 2,3-dioxygenase 1; COX-2, cyclooxygenase-2; GAPDH, glyceraldehyde-3-phosphate dehydrogenase; DCs, dendritic cells; DAMP, damage-associated molecular pattern.

stimulant of ROS production and tumor suppression, we further sought to determine whether addition of celecoxib could increase the ICD induced by GEM. Both GEM and celecoxib treatment increased activation of DCs compared to DMSO, and the GC group exhibited greater numbers of mature DCs compared to the other groups (*Figure 3A-3C*). Similarly, the phagocytic activity of DCs was enhanced by treatment with GEM or celecoxib compared to treatment with DMSO, and the best activity was observed in the GC group (*Figure 3D-3F*). In contrast to previous research (14), which reported CRT expression to be dependent on ROS-based ER stress, we observed no significant difference between the GEM and GC groups in the expression of CRT despite higher levels of ROS in the GC group compared to the GEM group. Similar results were observed for HSP90 (*Figure 3G*). As shown in *Figure 3G*, celecoxib counteracted the stimulatory effect of GEM, with lower expression of IDO1 in the GC group compared to the

GEM group. Consistent with this viewpoint, the addition of celecoxib dramatically enhanced the level of ROS compared to the addition of GEM alone. The effective immunogenicity induced by GC may therefore be partially due to ROS-based ER stress.

Combination therapy-induced tumor cell immunogenicity by inhibiting the PI3K/AKT signaling pathway

Accumulating evidence suggests that certain types of chemotherapeutic agents induce tumor cell death and an inflammatory response, which subsequently activates adaptive antitumor immunity (15). In this study, we found that after treatment with GEM and celecoxib, P-PI3K and P-AKT protein levels declined in cells, which was accompanied by increased apoptosis and ER stress. Activation of the PI3K/AKT pathway impaired apoptosis and ER stress caused by GEM and celecoxib (*Figure 4A-4D* and Figure S3A-S3D), and activation of DCs was clearly suppressed (*Figure 4E,4F* and Figure S3E,S3F). Consequently, further analysis of the PI3K/AKT pathway, ER stress, DAMPs, and IDO1 was conducted. The addition of SC-79, an AKT agonist, had no significant effect on the expression of DAMPs, indicating that there was no relationship between the enhanced ICD induced by celecoxib and the protein levels of DAMPs (*Figure 4G* and Figure S3G). Furthermore, a similar result was obtained for IDO1, suggesting that DCs were effectively activated due to lack of immunosuppression by IDO1 (*Figure 4G* and Figure S3G). The expression of ER stress-related proteins declined after addition of SC-79, implying that ER stress partially contributed to the enhanced ICD effect (*Figure 4H* and Figure S3H). Overall, we demonstrated that the enhanced ICD induced by celecoxib was a consequence of increased ER stress and the downregulation of IDO1.

Role of CD8+ T cells in the antitumor effect elicited by GEM-celecoxib combination therapy

Previous study has indicated that enhanced activation and antigen presentation by DCs can promote adaptive immunity, with $CD8^+$ T cells being a prerequisite for this effect (16). Therefore, we used anti-CD4 monoclonal antibodies (aCD4s) and anti-CD8 monoclonal antibodies (aCD8s) to determine the specific cell type. As shown in *Figure 5A-5I*, concurrent administration of GEM and celecoxib significantly delayed tumor growth. Addition of aCD8 restored growth of the subcutaneous xenograft, but there was no obvious difference between the GC group and the GCP group. A similar pattern was observed for the combination of DOX and celecoxib. The results demonstrated that application of aCD4 or aCD8 effectively decreased the numbers of $CD4^+$ or $CD8^+$ T cells (*Figure 5J,5K*), and the number of mature DCs was increased by combinations of GEM and celecoxib or DOX and celecoxib (*Figure 5L,5M*). Overall, these results suggest that $CD8^+$ T cells played a crucial role in the GEM-celecoxib antitumor immunity.

Combination therapy with checkpoint inhibitors contributed to antitumor immunity

As a previous study reported, reactivation of T cells contributes to immune checkpoint blockade (ICB) therapy (17). In the results reported above, GC combination therapy enhanced the number of $CD8^+$ T cells. As observed in *Figure 6A,6B*, aPD-1 alone did not significantly delay tumor growth compared to PBS, while there was obvious suppression in the GEM, GC, and GCP groups. The best antitumor effect was obtained via treatment with GCP, which indicated that combination therapy with GC and aPD-1 synergistically destroyed the tumor. In addition, GCP combination therapy significantly prolonged survival as compared with treatment with PBS (*Figure 6C*). We subsequently used IHC to determine several proteins (*Figure 6D*). Compared with the PBS group, the GCP group showed reduced expression of COX-2 and IDO1, which was consistent with the *in vitro* data. Of particular note, levels of CD8 were significantly increased in the GCP group compared with the PBS group, indicating the viability of ICB therapy.

Subsequently, we found there were no differences in IL-2 levels among the groups, but the IL-10 levels in the GEM- and GCP-treated mice were somewhat lower, which may indicate reduced numbers of M2 macrophages (*Figure 6E,6F*). Additionally, there were no significant differences in $CD4^+$ T cells or $CD8^+IFN\text{-}\gamma^+$ cells among the groups. The GCP group showed a decrease in the number of $CD8^+$ T cells compared with the PBS group, which is in line with our abovementioned results. Furthermore, we found that the number of myeloid-derived suppressor cells (MDSCs) was significantly reduced in the GCP group compared to the PBS group (*Figure 6G-6J*).

GCP resulted in long-lasting antitumor immunity and systemic antitumor immunity against distal metastasis

Our data suggested that the combination therapy exhibited

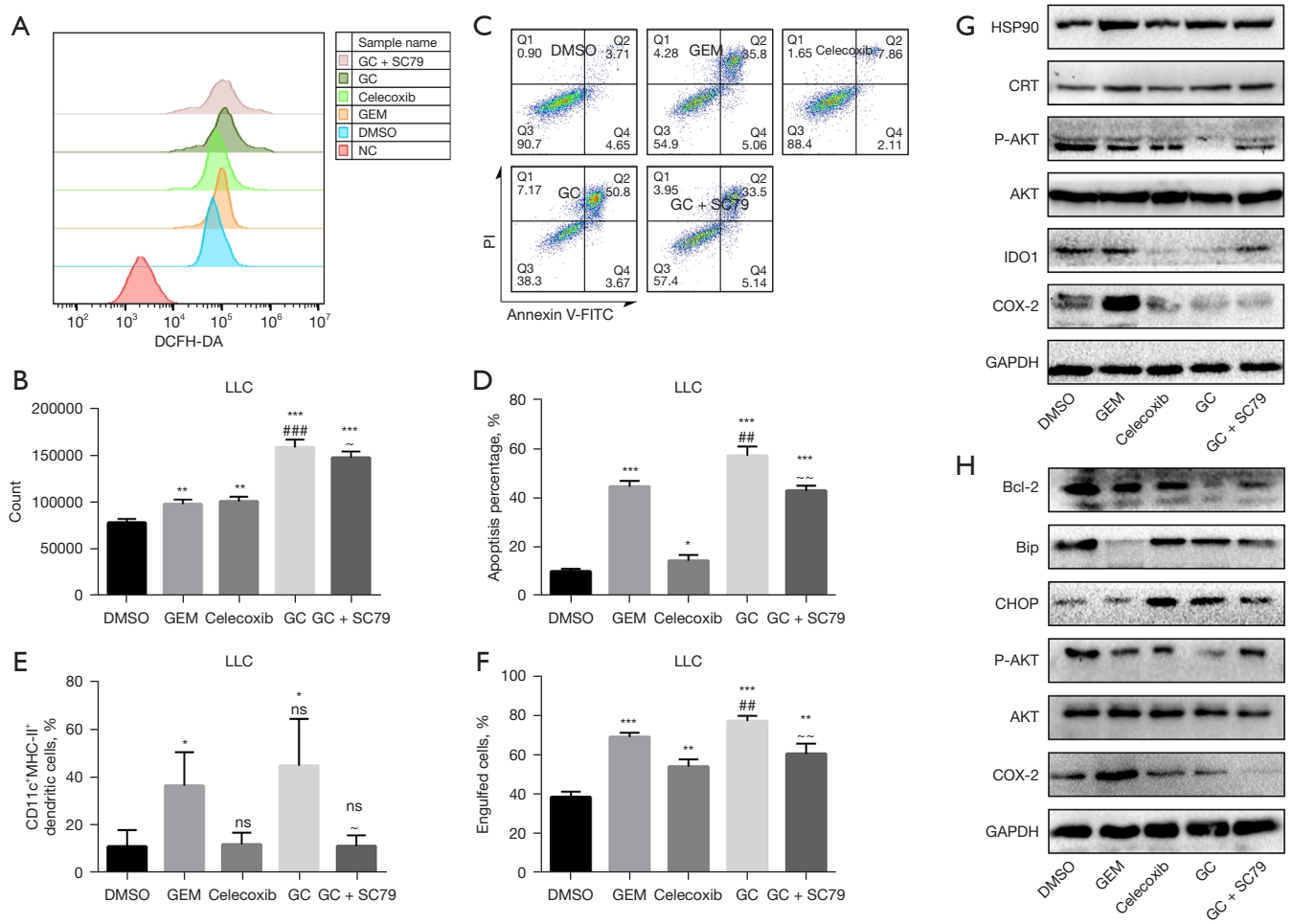

Figure 4 The molecular mechanism of celecoxib enhancement of GEM-induced ICD in LLC cells. Murine tumor cells (LLC) were treated with various agents (DMSO, GEM, celecoxib, GC, and GC + SC-79). (A,B) ROS levels were determined by using a ROS probe with flow cytometry. (C,D) An annexin V-FITC/PI kit was used to label apoptotic cells and was followed by flow cytometry. (E,F) The differences between various group in the activation of DCs (maturation and phagocytosis) were tested via flow cytometry. (G) Expression of ER stress-related proteins, IDO1, and others were measured via WB. (H) An AKT agonist was used to activate the PI3K/AKT pathway, and WB was performed to analyze the expression of related proteins. *, P<0.05, **, P<0.01, ***, P<0.001, compared with the DMSO group; ##, P<0.01, ###, P<0.001, GC group compared with the GEM group; ˜, P<0.05, ˜˜, P<0.01, GC + SC-79 group compared with the GC group; ns, P>0.05. DCFH-DA, 2,7-dichloro-dihydro-fluorescein diacetate; GC, GEM + celecoxib; GEM, gemcitabine; DMSO, dimethyl sulfoxide; NC, normal control; LLC, Lewis lung carcinoma; FITC, fluorescein isothiocyanate; PI, propidium iodide; MHC, major histocompatibility complex; HSP90, heat shock protein 90; CRT, calreticulin; P-, phospho-; IDO1, indoleamine 2,3-dioxygenase 1; COX-2, cyclooxygenase-2; GAPDH, glyceraldehyde-3-phosphate dehydrogenase; ICD, immunogenic cell death; ROS, reactive oxygen species; DCs, dendritic cells; ER, endoplasmic reticulum; WB, western blotting.

a synergistic antitumor effect. Although the proportion of tumor recurrence was not significantly reduced in the GCP group, it did decrease to a degree (Figure S4A,S4B). This suggests that long-term immunological antitumor memory could be induced by GCP treatment. We then evaluated effects of combination therapy on distal metastasis (Figure S4C-S4E). The lungs in the PBS group were almost completely covered with metastases, while those in the GCP group had less metastasis, suggesting that GCP treatment may activate a systemic antitumor immune response.

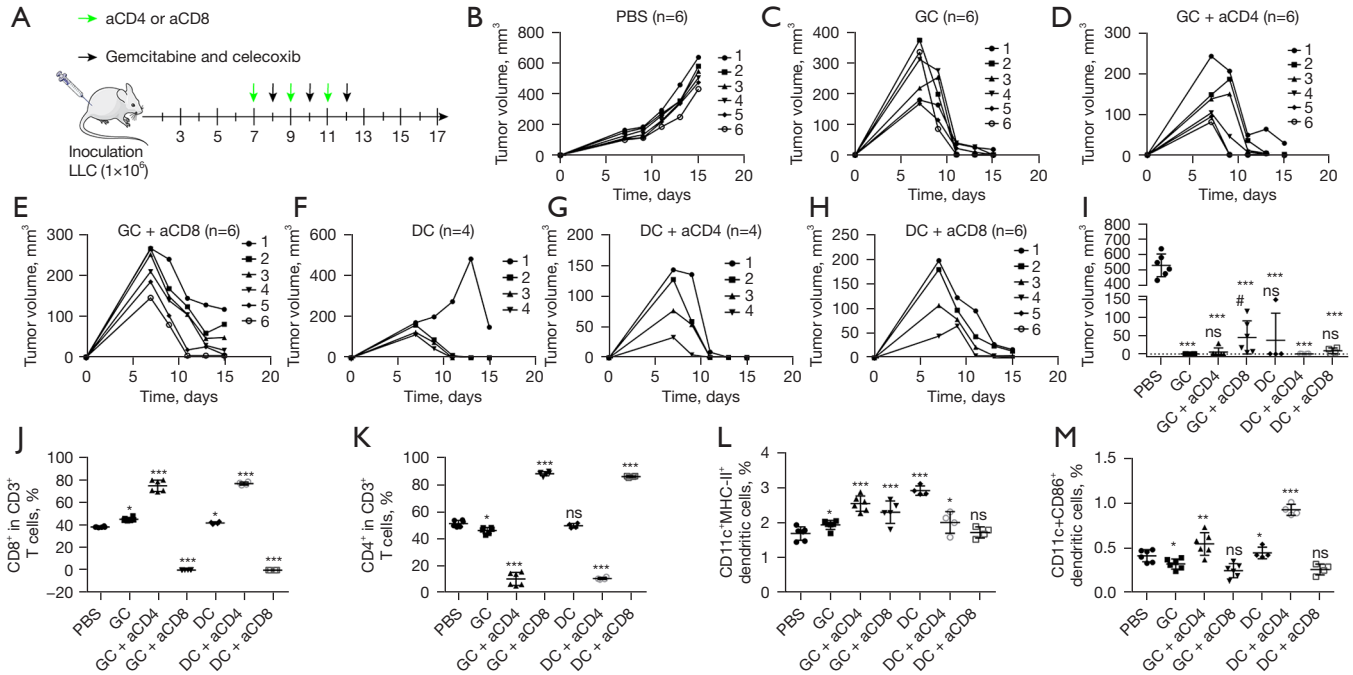

Figure 5 CD8$^+$ T cells play a crucial role in antitumor immunity. (A) Schematic diagram of an assay for investigating the specific cell mechanism of the combination of GEM and celecoxib in LLC tumor-bearing mice. C57 BL/6J mice were transplanted with LLC cells and injected with various agents (GEM, DOX, celecoxib, aCD4, and aCD8) at the indicated time points. Tumor volume in each group was calculated as described. (B-H) Tumor growth curves in individual mice are shown, and (I) data are presented as the mean ± SEM. (J-M) Immune cells were determined via flow cytometry. *, P<0.05, **, P<0.01, ***, P<0.001, compared with the PBS group; $^{\#}$, P<0.05, GC group compared with the GEM group or DC group compared with the DOX group; ns, P>0.05. In (B-H), each lines represent the tumor volume size of six different mice in each group at different time points. aCD4, anti-CD4 monoclonal antibody; aCD8, anti-CD8 monoclonal antibody; LLC, Lewis lung carcinoma; PBS, phosphate-buffered saline; GC, GEM + celecoxib; GEM, gemcitabine; DC, dendritic cell; MHC, major histocompatibility complex; DOX, doxorubicin; SEM, standard error of the mean.

Discussion

Over the recent decades, lung cancer has been the most frequent cause of cancer-related death worldwide (18). To further exploit the indications of existing chemotherapeutic agents, it is necessary to study their role in other aspects, including immunity. ICD is a particular mode of cell death observed during tumor immunogenicity and is different from apoptosis (19). This phenomenon can be stimulated by certain chemotherapeutic agents. In the present study, we investigated the characteristics of ICD induced by GEM and confirmed the potency of a therapy GCP in a mouse model of lung cancer.

There is controversy over whether GEM, as common chemotherapeutic drug in clinical practice, is a qualified ICD inducer. A large number of studies have shown that GEM can act as a qualified ICD inducer in rejecting tumor rechallenge in melanoma and breast cancer (20-22). Intriguingly, a recent study found GEM to act as a non-ICD inducer (23), but it is believed that the main reason preventing GEM from becoming a qualified ICD inducer is that GEM induces tumor cells to release PGE2, leading to the polarization of immunostimulatory DAMPs to inhibitory DAMPs. In our study, GEM was found to induce the production of DAMPs, and mice vaccinated with GEM-treated LLC cells were protected from rechallenge with LLC cells.

IDO1 seems to occupy a key role in the maturation and function of DCs. It has been reported that PGE2 released from tumor cells can activate β-catenin to induce IDO1 expression by activating the PI3K/AKT signaling pathway (24). PGE2 is an effective inducer of IDO1 expression in antigen-presenting cells, and continuous stimulation of PGE2 can induce IDO1 expression and

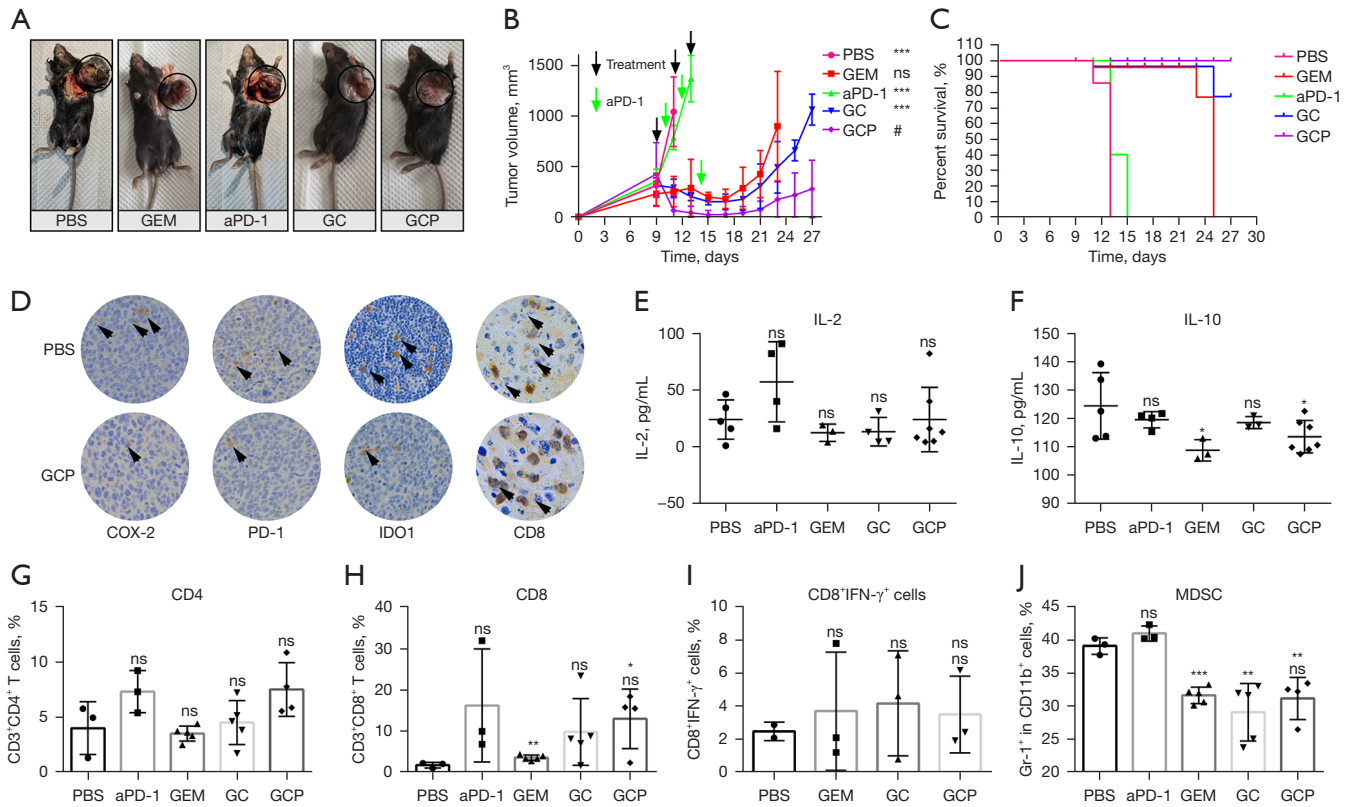

Figure 6 Combined therapy with aPD-1 enhanced the antitumor effect. LLC tumor-bearing C57 BL/6J mice were injected with PBS, GEM, aPD-1 alone, or in combination (GC and GCP). (A) A representative tumor was photographed. (B) Tumor volume was monitored at the indicated time. The data are expressed as the mean ± SEM, and the tumor growth curves of individual mice are shown. (C) Survival of tumor-bearing mice following treatments was recorded. (D) IHC analyses of several indicators (COX-2, PD-1, IDO1, and CD8) were conducted, cell images for 400× magnification under the light microscope, arrows indicated the positive cells. (E,F) Cytokines (IL-2 and IL-10) in peripheral blood were measured via ELISA after termination of the *in vivo* antitumor assay. (G-J) Several critical immune cells were investigated posttreatment via flow cytometry. *, P<0.05, **, P<0.01, ***, P<0.001, compared with the PBS group; #, P<0.05, GCP group compared with GC group; ns, P>0.05. PBS, phosphate-buffered saline; GEM, gemcitabine; aPD-1, anti-programmed death 1 monoclonal antibody; GC, GEM + celecoxib; GCP, GEM, celecoxib, and aPD-1; COX-2, cyclooxygenase-2; PD-1, programmed death 1; IDO1, indoleamine 2,3-dioxygenase 1; IL, interleukin; IFN, interferon; MDSC, myeloid-derived suppressor cell; SEM, standard error of the mean; IHC, immunohistochemistry; ELISA, enzyme-linked immunosorbent assay.

inhibit antitumor immunity (12). In our study, in order to prevent the inhibitory effect of PGE2 on ICD induced by GEM, celecoxib was added to the treatment regimen. As expected, attenuated expression of COX-2 was observed after the addition of celecoxib, along with decreased expression of IDO1, preventing the weakening of GEM-induced ICD.

Previous studies found that more severe ER stress can lead to higher ICD (25,26). Direct ROS-based ER stress is more effective for induction of ICD than is secondary collateral ER stress. In this study, the results indicated the augmentation of ROS-based ER stress following addition of celecoxib. Previous research has suggested that simultaneous induction of ER stress could restore and enhance the immunogenicity induced by therapeutic agents that are poor ICD inducers, such as etoposide and mitomycin C (2). Consistent with previous reports, we demonstrated the more potent induction of ICD via the combination of GEM with celecoxib compared to GEM alone due to more focused ER stress and higher levels of ROS. Furthermore, we observed a marked decrease of IDO1 expression after incubation with celecoxib. These

findings suggest that GEM-induced ICD could be enhanced by addition of celecoxib through aggravation of ER stress and reduction of IDO1 expression but not by increasing expression of DAMPs. In agreement with prior study, which reported that GEM and celecoxib suppress the PI3K/AKT signaling pathway (27), KEGG pathway analysis indicated GEM-treated cells were mainly affected in the process of that signal transduction. Moreover, we found celecoxib could reduce the production of PGE2 by inhibiting COX-2, further inactivating the PI3K/AKT pathway and eventually leading to decreased IDO1 expression. In subsequent experiments, we found that the portion of apoptotic cells, as well as DC activation and phagocytosis, was reduced in the GC group after the addition of SC-79. These results suggest that the combination of GEM and celecoxib promotes cell death by suppressing the PI3K/AKT signaling pathway. Moreover, the combination enhanced ICD by inducing ER stress and inhibiting IDO1 expression.

Prophylactic vaccines are the gold standard for assessment of ICD inducers (28). In our study, GEM-treated LLC cells exhibited potent immunogenicity, inducing strong antitumor immunity that was confirmed by successful protection of immunocompetent mice pretreated with GEM-treated LLC cells from rechallenge with parental LLC cells. Further investigation in central memory T cells ($CD3^+CD4^+CD62L^-$) indicated that GEM-treated cells stimulated immune memory function and prevented tumor cells from reinvasion. In agreement with previous study (29), our *in vivo* data further demonstrated that the combination of GEM and celecoxib ameliorated the local immunosuppressive state by increasing the proportions of $CD8^+$ T cells and mature DCs. We speculated whether a synergistic antitumor effect could be obtained using GCP. Consistent with a previous study (30), the addition of aPD-1 markedly enhanced antitumor efficacy and conferred long-lasting antitumor immunity. Robust antitumor immunotherapeutic efficacy is partially dependent on the enrichment of $CD8^+$ T cells that mediate tumor clearance (1).

In summary, we identified GEM as a qualified inducer of ICD that is able to ameliorate the immunosuppressive microenvironment in a model of lung cancer. Accumulating data support the viability and potential of the GCP for the treatment of lung cancer. However, these conclusions require further investigation for clinical efficacy to be established.

Conclusions

In summary, our study demonstrated that GEM can induce ICD in lung cancer cells, combination with celecoxib has potential to synergistically enhance the anti-tumor immunotherapy effect. Thus, we hypothesize that the GCP has promising clinical applications and may contribute to future synergistic multidrug anticancer treatments.

Acknowledgments

Funding: This work was supported by grants from the Science and Technology Foundation of Guangdong Province (No. 2021A1515010793 to Y.Z.), the Science and Technology Program of Guangzhou City (No. 202201020097 to Y.Z. and No. 2023A04J1200 to X.Z.), the Affiliated Cancer Hospital & Institute of Guangzhou Medical University (No. 2020-YZ-01 to Y.Z.), Wu Jieping Medical Foundation (No. 320.6750.2023.19-9), and the Plan on Enhancing Scientific Research in GMU to X.Z.

Footnote

Reporting Checklist: The authors have completed the ARRIVE and MDAR reporting checklists. Available at https://tcr.amegroups.com/article/view/10.21037/tcr-24-698/rc

Data Sharing Statement: Available at https://tcr.amegroups.com/article/view/10.21037/tcr-24-698/dss

Peer Review File: Available at https://tcr.amegroups.com/article/view/10.21037/tcr-24-698/prf

Conflicts of Interest: All authors have completed the ICMJE uniform disclosure form (available at https://tcr.amegroups.com/article/view/10.21037/tcr-24-698/coif). X.Z. reports that this work was supported by grants from the Science and Technology Program of Guangzhou City (No 2023A04J1200) and the Plan on Enhancing Scientific Research in GMU. Y.Z. reports that this work was supported by grants from the Science and Technology Foundation of Guangdong Province (No. 2021A1515010793), the Science and Technology Program of Guangzhou City (No. 202201020097), and the Affiliated Cancer Hospital & Institute of Guangzhou Medical University (No. 2020-YZ-01). L.L. and C.C. are from Guangzhou Youdi Bio-Technology Co., Ltd., Guangzhou, China. D.P. is from Acobiom, Montpellier, France. The other authors have no conflicts of interest to declare.

Ethical Statement: The authors are accountable for all

aspects of the work in ensuring that questions related to the accuracy or integrity of any part of the work are appropriately investigated and resolved. All animal experiments were approved by the Animal Care and Use Committee of Southern Medical University (No. LAEC-2020-049). The welfare of live experimental animals was maintained in strict accordance with the Ministry of Science and Technology (2006) No. 398 Guidelines for the Treatment of Experimental Animals for the care and use of animals.

References

1. Ahmed A, Tait SWG. Targeting immunogenic cell death in cancer. Mol Oncol 2020;14:2994-3006.
2. Krysko DV, Garg AD, Kaczmarek A, et al. Immunogenic cell death and DAMPs in cancer therapy. Nat Rev Cancer 2012;12:860-75.
3. Ma J, Ramachandran M, Jin C, et al. Characterization of virus-mediated immunogenic cancer cell death and the consequences for oncolytic virus-based immunotherapy of cancer. Cell Death Dis 2020;11:48.
4. Legrand AJ, Konstantinou M, Goode EF, et al. The Diversification of Cell Death and Immunity: Memento Mori. Mol Cell 2019;76:232-42.
5. Li Q, Liu J, Fan H, et al. IDO-inhibitor potentiated immunogenic chemotherapy abolishes primary tumor growth and eradicates metastatic lesions by targeting distinct compartments within tumor microenvironment. Biomaterials 2021;269:120388.
6. Song X, Zhou Z, Li H, et al. Pharmacologic Suppression of B7-H4 Glycosylation Restores Antitumor Immunity in Immune-Cold Breast Cancers. Cancer Discov 2020;10:1872-93.
7. Xiang Y, Chen L, Li L, et al. Restoration and Enhancement of Immunogenic Cell Death of Cisplatin by Coadministration with Digoxin and Conjugation to HPMA Copolymer. ACS Appl Mater Interfaces 2020;12:1606-16.
8. Dong S, Guo X, Han F, et al. Emerging role of natural products in cancer immunotherapy. Acta Pharm Sin B 2022;12:1163-85.
9. Zheng M, Zhang W, Chen X, et al. The impact of lipids on the cancer-immunity cycle and strategies for modulating lipid metabolism to improve cancer immunotherapy. Acta Pharm Sin B 2023;13:1488-97.
10. Ouyang Y, Zhong W, Xu P, et al. Tumor-associated neutrophils suppress CD8(+) T cell immunity in urothelial bladder carcinoma through the COX-2/PGE2/IDO1 Axis. Br J Cancer 2024;130:880-91.
11. Shi Y, Lammers T. Combining Nanomedicine and Immunotherapy. Acc Chem Res 2019;52:1543-54.
12. Balamurugan K, Poria DK, Sehareen SW, et al. Stabilization of E-cadherin adhesions by COX-2/GSK3β signaling is a targetable pathway in metastatic breast cancer. JCI Insight 2023;8:e156057.
13. Srivastava S, Dewangan J, Mishra S, et al. Piperine and Celecoxib synergistically inhibit colon cancer cell proliferation via modulating Wnt/β-catenin signaling pathway. Phytomedicine 2021;84:153484.
14. Li W, Yang J, Luo L, et al. Targeting photodynamic and photothermal therapy to the endoplasmic reticulum enhances immunogenic cancer cell death. Nat Commun 2019;10:3349.
15. Guo J, Zou Y, Huang L. Nano Delivery of Chemotherapeutic ICD Inducers for Tumor Immunotherapy. Small Methods 2023;7:e2201307.
16. Ye J, Mills BN, Zhao T, et al. Assessing the Magnitude of Immunogenic Cell Death Following Chemotherapy and Irradiation Reveals a New Strategy to Treat Pancreatic Cancer. Cancer Immunol Res 2020;8:94-107.
17. Pan Y, Kadash-Edmondson KE, Wang R, et al. RNA Dysregulation: An Expanding Source of Cancer Immunotherapy Targets. Trends Pharmacol Sci 2021;42:268-82.
18. Leiter A, Veluswamy RR, Wisnivesky JP. The global burden of lung cancer: current status and future trends. Nat Rev Clin Oncol 2023;20:624-39.
19. Yu S, Xiao H, Ma L, et al. Reinforcing the immunogenic cell death to enhance cancer immunotherapy efficacy. Biochim Biophys Acta Rev Cancer 2023;1878:188946.
20. Zhou S, Shang Q, Wang N, et al. Rational design of a minimalist nanoplatform to maximize immunotherapeutic efficacy: Four birds with one stone. J Control Release 2020;328:617-30.
21. Gebremeskel S, Lobert L, Tanner K, et al. Natural

Killer T-cell Immunotherapy in Combination with Chemotherapy-Induced Immunogenic Cell Death Targets Metastatic Breast Cancer. Cancer Immunol Res 2017;5:1086-97.
22. Wang C, Wang J, Zhang X, et al. In situ formed reactive oxygen species-responsive scaffold with gemcitabine and checkpoint inhibitor for combination therapy. Sci Transl Med 2018;10:eaan3682.
23. Hayashi K, Nikolos F, Chan KS. Inhibitory DAMPs in immunogenic cell death and its clinical implications. Cell Stress 2021;5:52-4.
24. Hennequart M, Pilotte L, Cane S, et al. Constitutive IDO1 Expression in Human Tumors Is Driven by Cyclooxygenase-2 and Mediates Intrinsic Immune Resistance. Cancer Immunol Res 2017;5:695-709.
25. Feng X, Lin T, Chen D, et al. Mitochondria-associated ER stress evokes immunogenic cell death through the ROS-PERK-eIF2α pathway under PTT/CDT combined therapy. Acta Biomater 2023;160:211-24.
26. Janssens S, Rennen S, Agostinis P. Decoding immunogenic cell death from a dendritic cell perspective. Immunol Rev 2024;321:350-70.
27. Liu B, Yan S, Qu L, et al. Celecoxib enhances anticancer effect of cisplatin and induces anoikis in osteosarcoma via PI3K/Akt pathway. Cancer Cell Int 2017;17:1.
28. Wang Z, Chen J, Hu J, et al. cGAS/STING axis mediates a topoisomerase II inhibitor-induced tumor immunogenicity. J Clin Invest 2019;129:4850-62.
29. Liu X, Cen X, Wu R, et al. ARIH1 activates STING-mediated T-cell activation and sensitizes tumors to immune checkpoint blockade. Nat Commun 2023;14:4066.
30. Hayashi K, Nikolos F, Lee YC, et al. Tipping the immunostimulatory and inhibitory DAMP balance to harness immunogenic cell death. Nat Commun 2020;11:6299.

Cite this article as: Zhu X, Zhang W, Yu Z, Yang X, Li L, Chen C, Djumanazarov T, Piquemal D, Yusupbekov AA, Zheng Y. Synergistic action of gemcitabine and celecoxib in promoting the antitumor efficacy of anti-programmed death-1 monoclonal antibody by triggering immunogenic cell death. Transl Cancer Res 2024;13(6):3031-3045. doi: 10.21037/tcr-24-698

